Triple molecular target approach to selective melanoma cytotoxicity†

Edward B. Skibo,* Akmal Jamil, Brittany Austin, Douglas Hansen and Armand Ghodousi

Received 29th September 2009, Accepted 21st December 2009
First published as an Advance Article on the web 28th January 2010
DOI: 10.1039/b920260a

Phenylalanine-linked pyrrolo[1,2-*a*]benzimidazoles were successfully designed to target melanoma cells *in vitro*. Our design utilised three molecular targets: a phenylalanine pump, the reducing enzyme DT-diaphorase, and IMP dehydrogenase. We describe the synthesis of these compounds as well as the results of *in vitro*, *in vivo*, and QSAR studies.

Introduction

A molecular target is a protein or enzyme that is highly expressed in human tumour cell lines. The levels of over one thousand biologically relevant molecular targets have been determined in human tumour cell lines from measurements of mRNA and enzyme activity levels.[1] A therapeutic agent directed toward one or more of these molecular targets has the potential of exhibiting cancer-cell selectivity. A classic molecular target is the quinone two-electron reducing enzyme DT-diaphorase. The unusually high expression of DT-diaphorase in some histological cancer types[2–6] contributes to the tumour's tendency to reduce quinones. The clinically used quinone-based antitumour agent mitomycin C is a well known example of an alkylating agent activated by DT-diaphorase (*i.e.* a bioreductive-alkylating agent).[7–11] Selective bioreductive alkylation in high DT-diaphorase cancer types (melanoma, renal and non-small-cell lung cancers)[1] would exhibit maximal antitumour activity with minimal side effects.

Our hypothesis is that a structure utilising three molecular targets, rather than just one, would possess a high degree of histologic specificity. We chose to design a melanoma-specific structure utilising the L-phenylalanine pump found in melanocytes[12] as well as the elevated levels of both DT-diaphorase and inosine monophosphate dehydrogenase (IMPDH) found in melanoma cells.[1] Upon uptake by the L-phenylalanine, reductive activation by DT-diaphorase would then be followed by the inactivation of IMPDH. Fig. 1 shows the structure designed to utilise three molecular targets. This structure possesses a phenylalanine dipeptide portion that is designed to play a role in uptake of the compound into the melanoma cell as well as to promote IMPDH binding.

The pyrrolo[1,2-*a*]benzimidazole (PBI) ring system shown in Fig. 1 possesses the benzimidazole ring system designed to mimic the hypoxanthine ring of the inosine monophosphate (IMP) substrate of IMPDH. The PBI ring system is functionalised as an aziridinylquinone to provide bioreductive alkylation capability. The synthesis and biological properties of PBI derivatives have been extensively documented by this laboratory.[13–22]

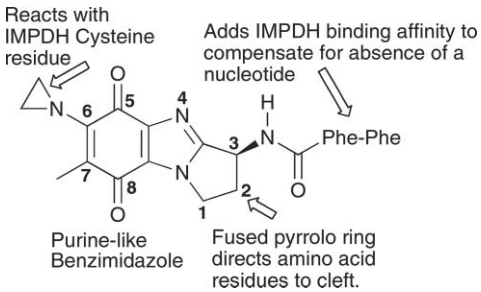

Fig. 1 Design features of the structure utilising three molecular targets. IUPAC numbering of the pyrrolo[1,2-*a*]benzimidazole ring is shown.

Inosine monophosphate dehydrogenase (IMPDH) is responsible for nicotinamide adenine dinucleotide (NAD)-dependent oxidation of IMP to xanthine monophosphate (XMP), which is the rate-limiting step in the guanosine monophosphate (GMP) biosynthetic pathway.[23,24] Human inosine monophosphate dehydrogenase exists in two isoforms type I and II, but type II is considered a more important target in chemotherapeutic design since this isoform is up-regulated in neoplastic cells and is the predominant form.[25] IMPDH inhibitors possess a broad spectrum of biological activity including antitumour, immunosuppression, antiviral, and antibacterial activity.[23,25,26] This broad spectrum of activity reflects the importance of GMP in diverse biological pathways. Therefore, the proposed IMPDH inhibitor shown in Fig. 1 was expected to exert cytostatic and cytotoxic activity on melanoma cells.

Known IMPDH inhibitors usually mimic either the enzyme's IMP or NAD substrates.[27] Mycophenolic acid, which binds to the NAD cofactor site, represents the earliest inhibitors of IMP dehydrogenase. Bredinin and ribavirin[28,29] are two examples of nucleoside-based inhibitors that bind in the IMP site of the enzyme upon their metabolic conversion to the 5′-monophosphate form. Selenazofurin and benzamide riboside[30] are potent inhibitors of inosine monophosphate dehydrogenase that binds in the NAD site of the enzyme upon metabolic conversion to the corresponding NAD analogue. With crystal structures of IMPDH in hand, it has been possible to design non-nucleotide inhibitors.[31–34,35,36] Similarly, we used reported crystal structures of human IMPDH type II (Protein Data Bank # 1B30)[37] to aid in our IMPDH inhibitor design.

Department of Chemistry and Biochemistry, Arizona State University, Tempe, Arizona 85287-1604. E-mail: eskibo@asu.edu; Fax: +1 480 965 2747; Tel: +1 480 965 3581

† Electronic supplementary information (ESI) available: Spectroscopic data for all compounds and *in vitro* assay results. See DOI: 10.1039/b920260a

Results and discussion

IMPDH inhibitor design

In 1980, one of us (EBS) designed phenyl-substituted IMP analogues that exhibited enhanced binding to the IMP binding site by taking advantage of a hydrophobic pocket located at the 8-position of the purine ring.[38] The actual presence of the pocket was verified by crystal structures obtained many years later.[39] In 2004, COMPARE analysis of 60-cancer cell line mean graph data for a substituted PBI analogue revealed that IMPDH was its molecular target.[22] The COMPARE analysis correlates mean graph data with known molecular target levels in cell lines and thereby generate hypotheses concerning the agent's mechanism of action.[40,41] Considering the aforementioned results, we postulated that substituted PBIs could exploit the hydrophobic pocket located at the 8-position of the purine ring

The model used to design these inhibitors was developed by superimposing the benzimidazole ring of the L-phenylalanine-linked pyrrolobenzimidazole system unto the purine ring of active site bound 6-ChloroIMP. After the superimposition, the active site IMP structure is subtracted from the model and the active site bound pyrrolobenzimidazole and enzyme complex minimised to afford the structure shown in Fig. 2. This structure shows that the amino acid residue of the PBI occupies a cleft different than that occupied by the ribofuranosyl and phosphate residues of the IMP substrate. The pyrrolo ring of the pyrrolobenzimidazole ring system, as well as the *S*-stereochemistry of the 3-position, directs the amino acid residues to this cleft. Modeling studies revealed that the L-phenylalanine (the *S*-enantiomer) binds more tightly than the D-form (the *R*-enantiomer). Modelling the hydroquinone derivative of the PBI into the IMPDH active site afforded a structure similar to that shown in Fig. 2. These modelling studies showed that a PBI-based inhibitor, either as the quinone or hydroquinone, could bind to the IMPDH active site.

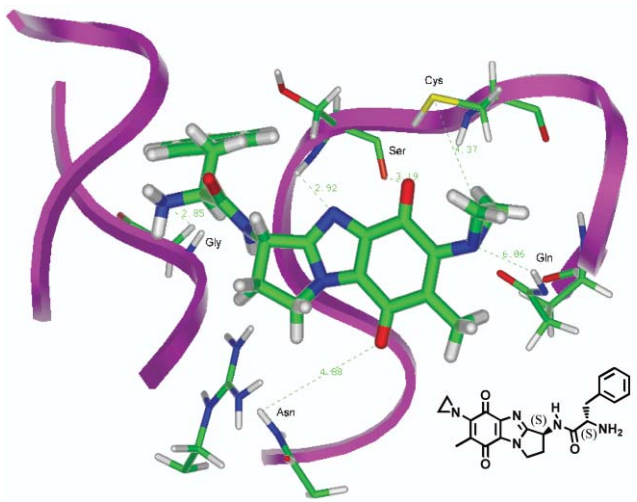

Fig. 2 A PBI analogue modelled into the purine active site of human type II IMPDH.

Inspection of Fig. 2 also reveals that the aziridinyl group is proximal to an active site cysteine residue (sulfur shown in yellow). Reaction between these centres could occur with either the quinone or the hydroquinone forms of the PBI resulting in irreversible inactivation of IMPDH, Scheme 1. However, the aziridinyl hydroquinone form is expected to be a more reactive alkylating agent based on literature precedents.[14,42]

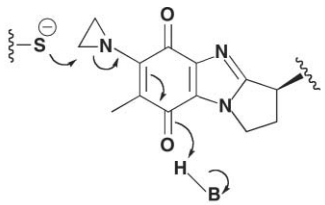

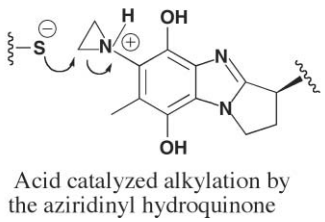

Scheme 1 Aziridinyl alkylation mechanisms.

PBI–phenylalanine analogue synthesis

The PBI-linked phenylalanine analogues prepared for this study are shown in Fig. 3 and 4. The diphenylalanine analogues **1** shown in Fig. 3 possess all four D- and L-stereochemical possibilities. The goal was to investigate the influence of stereochemistry on melanoma histological specificity and *in vivo* activity. According to our hypothesis, the D-enantiomers should possess diminished melanoma specificity. We also prepared the analogues **2** shown in Fig. 4 to investigate the role of aromatic substituents on histological specificity. The goal was to discover a PBI analogue linked to a substituted L-phenylalanine that still possesses melanoma specificity. A quantitative structure–activity relationship (QSAR) derived from *in vitro* data for analogues **2** would guide future analogue development.

We prepared **LD1**, **DL1**, and **DD1** using the synthetic methodology previously described for **LL1**.[22] Scheme 2 outlines the preparation PBI-linked phenylalanines **2** starting with 3-bromo-4-nitrotoluene **3**. The conversion of **3** to the (*S*)-amino pyrrolo[1,2-*a*]benzimidazole derivative **4** is a multistep process previously reported from this laboratory.[14,17,20,43,44] The substituted phenylalanine was coupled to the amine group of **4** employing dicyclohexyl carbodiimide (DCC). The coupling product **6** was subject to catalytic reduction to both remove the bromo group and reduce the nitro group to the amine. The amine was then subjected to Fremy oxidation to afford the quinone analogues **7**. Removal of the *t*-Boc followed by aziridination afforded the final products **2**.

Melanoma histological specificity of the diphenylalanine PBIs 1

The compound series **1** shown in Fig. 3 was screened against the National Cancer Institute's 60 cell line human cancer panel.[40,45–47] This panel consists of the nine major histological types of human cancers. We used the average –log LC_{50} values for each cancer

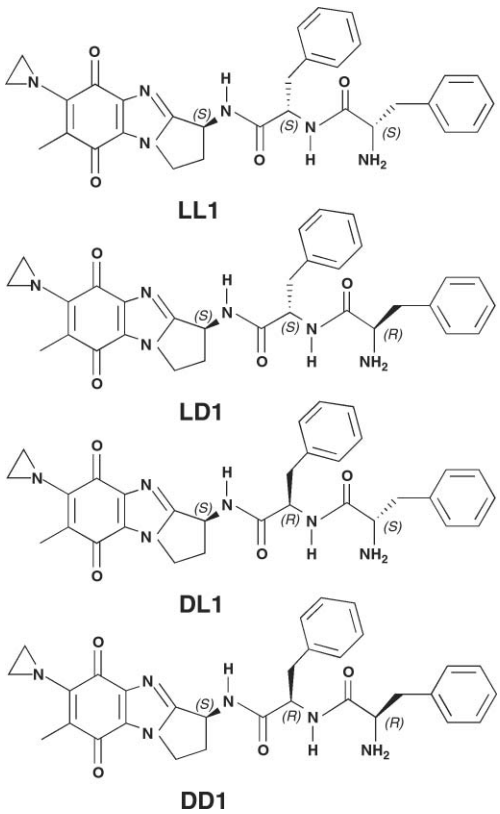

Fig. 3 Stereoisomers of diphenylalanine-linked PBIs **1** prepared for this study.

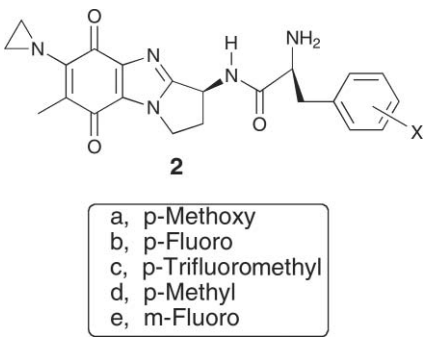

Fig. 4 Substituted L-phenylalanine-linked PBIs prepared for this study.

type to determine the sensitivity toward the stereoisomers of **1**. The LC_{50} value, the cytotoxicity parameter, is the concentration of agent at which there is 50% lethality toward the cancer cell line. The lower the LC_{50} value, the more potent the agent. Similarly, the larger the –log LC_{50} value, the more potent the agent. The bar graph in Fig. 5 shows the relative activity (–log LC_{50}) of the stereoisomers of **1** towards the NCI nine-cancer panel. The raw data used to obtain Fig. 5 is found in the Supplementary Information Section.

The stereoisomer **LL-1** possesses the expected high cytotoxic specificity toward the melanoma panel. Actually, many of the LC_{50} values for melanoma cell lines are $< 10^{-8}$ M, so the melanoma bar for **LL-1** in Fig. 5 is even higher. In contrast, the stereoisomer **LD-1** possesses diminished melanoma specificity. This observation is consistent with our hypothesis that the terminal L-phenylalanine

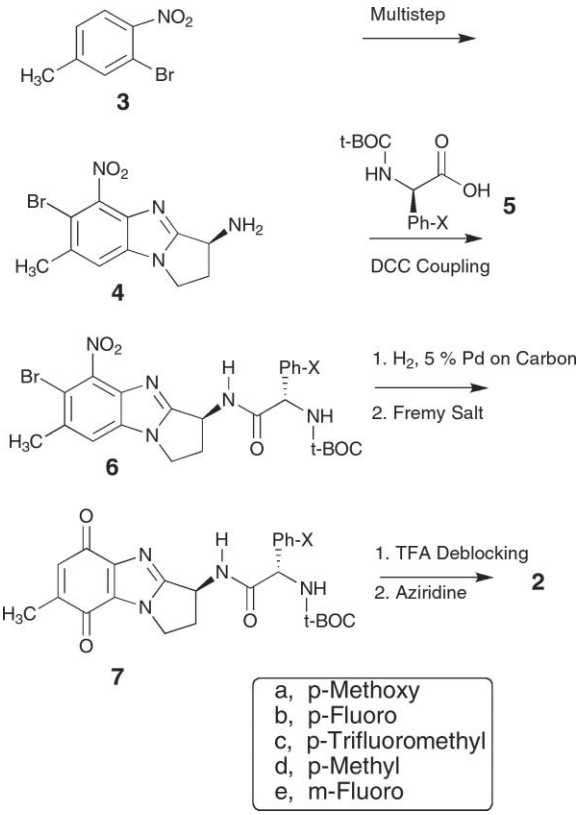

Scheme 2 Synthesis of the PBI-linked phenylalanines **2**.

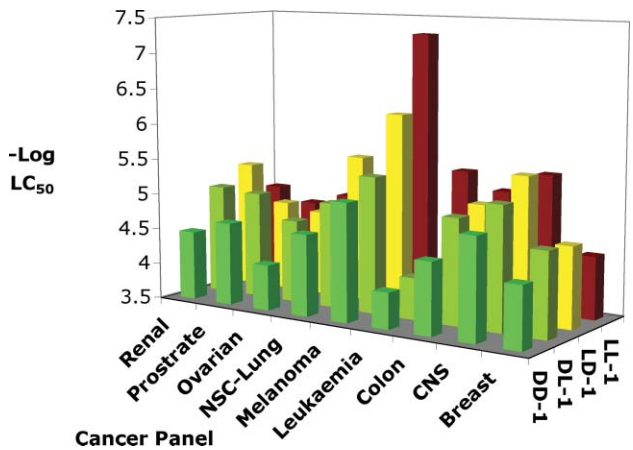

Fig. 5 Bar graph of the average –logLC_{50} values for series **1** plotted against nine cancer panels. Higher bars represent higher activity.

of **1** utilises an L-phenylalanine pump found in melanocytes[12] to gain entry into the melanoma cell.

The stereoisomers **DL-1** and **DD-1** possess a low level of cytotoxicity against all of the cancer panels. There is no apparent melanoma specific cytotoxicity for either of these stereoisomers. This result is consistent with our modelling studies that indicated the first phenylalanine must be L to be accommodated by the IMPDH active site.

The conclusion is the both phenylalanines of **1** must have the L stereochemistry for there to be melanoma specificity.

In vivo activity of LL-1 and LD-1

The *in vivo* activity of the most cytotoxic analogues **LL-1** and **LD-1** were evaluated in a xenograft human tumour model and in the National Cancer Institute's hollow fibre[48,49] assay respectively.

We assayed **LL-1** in the xenograft tumour model consisting of human lung tumour cells (NCI-H460) implanted into SCID mice. This readily available lung tumour model would primarily provide toxicity information as well as evidence of antitumour activity (**LL-1** exhibits cytostatic activity at nanomolar levels against a broad range of human cancers). Compound **LL-1** was administered intraperitoneally (IP) to SCID mice at doses of 1, 3, and 5 mg kg^{-1} at 4 day intervals for a total of six doses. We used a vehicle control and a mitomycin C treated control as references. Tumour growth inhibition was calculated at T/C (treated/control) × 100. T/C Values ≤ 42% are considered active, indicated with an * in Fig. 6 and 7. Inspection of Fig. 6 reveals that the 1 mg kg^{-1} dose did not reduce tumour mass compared to the control, but resulted in 3/6 animal deaths. In contrast, mitomycin C was active at all doses without animal deaths.

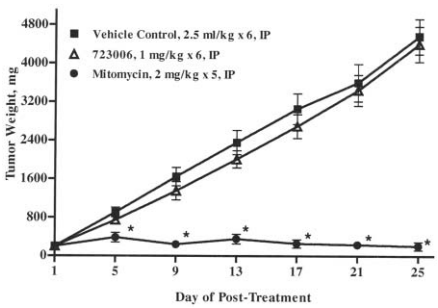

Fig. 6 The tumour growth curves in SCID mice for **LL1** (NSC # 723006), the vehicle control and the mitomycin C control.

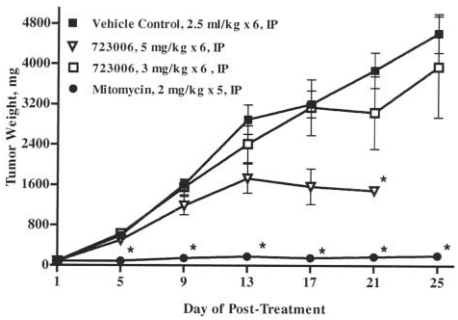

Fig. 7 The tumour growth curves in SCID mice are shown for **LL1** (NSC # 723006) at 2 and 5 mg kg^{-1}. The vehicle control and the mitomycin C control are also shown.

Fig. 7 shows that the 2 and 5 mg kg^{-1} doses for **LL-1** reduced tumour mass somewhat. The 5 mg kg^{-1} dose showed an active level of tumor reduction (37%) by the 5th dose. Animal survival continued to be a problem at these dosages with a 3/6 and 6/6 death rate for 2 and 5 mg kg^{-1} respectively. In conclusion **LL-1** possesses very little antitumor activity with toxicity even at low doses.

Compound **LD-1** was far less toxic than **LL-1** with a measured maximum tolerated dose (MTD) of 6.5 mg kg^{-1}. The hollow fiber assay of **LD-1** was carried out as previously described.[48,49] The hollow fibre score is broken down into a intraperitoneal (IP) and a subcutaneous (SC) score that is based on the percent of cancer left in the fiber (<50% = 2 and >50% = 0) The highest total score (IP + SC) is 96. The typical antitumor agent only has a hollow fiber score of ~5 while the highest score being 64 for the natural product cyclin-dependent kinase inhibitor flavopiridol.[50] A good SC score (≥ 8) indicates that the drug is able to get to the tumor site (subcutaneous) from a distant site (intraperitoneal) of injection. Compound **LD-1** had an IP score of 42/48 and an SC score of 2/48. These results indicate that compound **LD-1** has excellent antitumor activity in this assay. The hollow fibre scores shown in Table 1 reveals that **LD-1** even has higher activity than clinically used antitumor agents.

Table 1 Hollow fibre scores of **LD-1** and those of clinically used antitumour agents

Compound	Intraperitoneal (IP) score	Subcutaneous (SC) score	Total score
LD-1	42	2	44
Taxol	24	8	32
Cisplatin	14	8	22

The conclusion of the *in vivo* studies is that L-phenylalanine linked analogs are toxic and lack antitumour activity unless followed by D-phenylalanine as in **LD-1**. Enzymatic removal of one or both phenylalanines would afford the amino-substituted pyrrolobenzimidazole **8** that is known to be highly toxic due to its cleavage of DNA,[20] Scheme 3. Likewise, the L-phenylalanine-linked PBI **2f**[22] is highly toxic *in vivo* showing much the same results as **LL-1**.

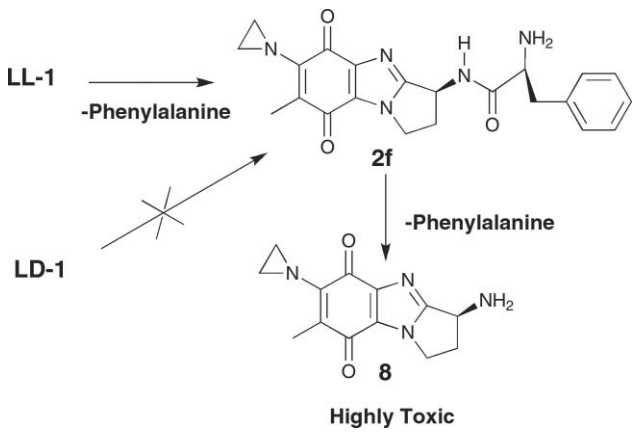

Scheme 3 Reactions that could be responsible for the high toxicity of **LL-1** and **2f** as well as the low toxicity of **LD-1**.

In contrast, the unnatural D-phenylalanine of **LD-1** is not likely subject to *in vivo* hydrolysis and the toxic metabolite **8** is never formed. However, the L-enantiomer of phenylalanine is preferred as far as melanoma specificity is concerned. The substituted analogues shown in Fig. 4 may circumvent hydrolytic removal of the L-enantiomer. Perhaps a substituent would render the L-phenylalanine "unnatural" and not susceptible to hydrolysis. Or perhaps the substituent will enhance melanoma specificity and cytotoxicity.

Table 2 Results of matrix COMPARE for compound series **2**. Pearson correlation coefficients are shown for each compound pair

	2f	2a	2b	2c	2d
2a	0.71				
2b	0.766	0.876			
2c	0.657	0.77	0.67		
2d	0.612	0.858	0.832	0.78	
2e	0.607	0.733	0.716	0.735	0.913

Matrix COMPARE of the monophenylalanines PBIs 2, melanoma histological specificity, and QSAR

The goal of these studies was to determine the L-phenylalanine substituent type that would optimise melanoma specificity and cytotoxicity. Compound series **2**, shown in Fig. 4, were screened against the National Cancer Institute's 60 cell line human cancer panel.[40,45–47] The raw data used to generate the results described below are found in the Supplementary Information Section.

We carried out a matrix COMPARE[40,46,51] by comparing pairwise the patterns of cytotoxicity against a 60 cell line human cancer panel for **2a–f**, Table 2. The substituted phenylalanine analogues **2a** and **2b** show the highest correlations with the analogue linked to unsubstituted L-phenylalanine **2f**. The data in Table 2 also indicate that the substituted phenylalanine analogues **2a–e** correlate well with each other (coefficients 0.7 to 0.9). These high correlations are expected given their structural similarity. The anomaly is the pair **2d** and **2e** that correlated well with each other (0.913), but not with the parent compound **2f** (~0.6). In fact, both compounds possess little melanoma specificity.

The bar graph in Fig. 8 shows the relative activity (–log LC_{50}) of **2a**,**b** and **2f**[22] towards the NCI nine-cancer panel. These results suggest that the *p*-methoxy and *p*-fluoro substituted L-phenylalanines of **2a**,**b** would be suitable mimics of natural L-phenylalanine. Inspection of the Fig. 8 reveals that **2a**,**b** and **2f** possess specificity toward the melanoma panel, although not as high as the diphenylalanine analogue **LL-1**. Fig. 5 shows that melanoma histological specificity requires the presence of two linked L-phenylalanines. The proposed second generation analogues will likewise consist of PBI linked to *p*-methoxy or *p*-fluoro substituted diphenylalanine.

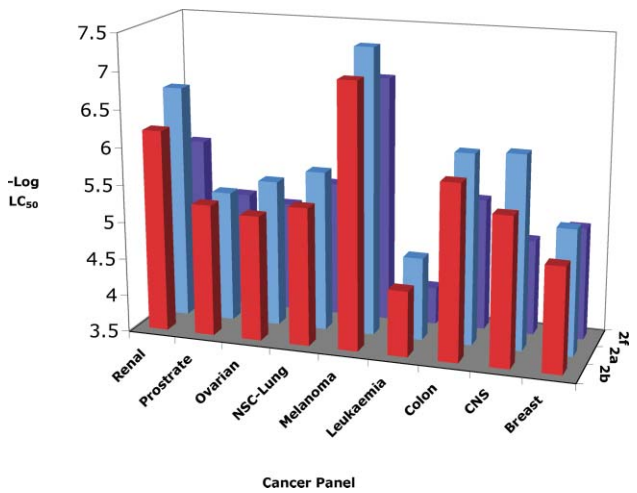

Fig. 8 Bar graph of the average –logLC_{50} values for **2a**,**b** and **2f** plotted against nine cancer panels. Higher bars represent higher activity.

Inspection of Fig. 8 reveals that the substituent influences the level of –log LC_{50} in the melanoma panel. We carried out a QSAR analysis[52] (quantitative structure activity relationship) to find the substituent type required for optimal activity against the melanoma panel. Substituent parameters used in the analysis include π (lipophilicity), σ (electron withdrawing/releasing), F (field, a measure of inductive electronic effects), and MR (molar refractivity, a measure of size and polarizability). Multivariable regression analysis provided the following relationship (R squared is 98%):

$$-\log LC_{50} = 0.48\pi + 0.61F - 1.52\sigma + 6.77 \quad (1)$$

The constant 6.77 is the –logLC_{50} of the unsubstituted analogue, the actual value is 6.81. This QSAR relationship shows that the preferred substituent is electron releasing (σ is negative) with an electron withdrawing inductive component (F is positive) and lipophilic character (π is positive). The *para*-methoxy substituent possesses most of these preferred characteristics: $\sigma = -0.27$, $F = 0.26$, and $\pi = -0.02$.[53] Other suitable substituents include the halogens and the *N*,*N*-dimethylamino group. At this time, we are screening these phenyl-substituted derivatives of **LL-1**. The limited number and type of substituents used to obtain this QSAR relationship prohibits its extension to very large and very lipophilic substituents.

COMPARE analysis

COMPARE analysis correlates mean graph data with known molecular target levels in cell lines and thereby generates hypotheses concerning the agent's mechanism of action. The levels of over one thousand biologically relevant molecular targets have been determined in these tumor cell lines from measurements of mRNA and enzyme activity levels.[1]

The observed specificity of **LL-1** and **2f** for the melanoma panel is likely related to specific cellular uptake. The events leading to cell death, reductive activation and IMPDH inhibition, occur down stream to the uptake process. The COMPARE analysis described below provides insights into what molecular targets might be involved in uptake.

COMPARE analysis of **2f** showed a good correlation (0.59) with ABC-B5, a gene for an ATP-binding membrane protein involved with substrate transport. This protein is expressed in melanoma cells as well as melanocytes[54] and is implicated in the resistance of malignant melanomas to doxorubicin.[55] Perhaps the ABC-B5 transporter is involved in the actual transport of compound **2f** into melanoma cells. However, COMPARE analyses of the D-stereoisomer of **2f** and the substituted analogues **2a–e** did not correlate with ABC-B5.

COMPARE analysis of **LL-1** showed a very good correlation with ECM1 (0.66), a gene for the Extracellular Matrix Protein 1. The level of this protein is associated with metastatic potential,[56] and shows elevated values only in the melanoma cell lines of the 60-cell line panel. We do not know if **LL-1** directly interacts with the ECM1 protein or if the correlation happens to be coincidental. COMPARE analysis of the D-stereoisomer (**DL-1**) showed loss of the ECM1 correlation as well as loss of melanoma specificity.

The conclusion of this section is that a L-phenylalanine is very likely required for melanoma specificity. A second generation derivative of **LL-1**, with a substituted L-phenylalanine and a terminal L-phenylalanine, could display melanoma specificity without toxicity.

IMPDH inhibition

These studies validate the modeling studies (Fig. 2) that predicted **2f** could interact with the IMPDH active site. In addition, these studies suggest that IMPDH could be a molecular target for compound series **2**.

The activity of human recombinant type II IMP dehydrogenase was determined by monitoring the absorbance of NADH that was formed during oxidation of inosine monophosphate (IMP) to xanthosine monophosphate (XMP). To carry out these assays, the concentration of IMP was varied while keeping the concentration of NAD constant. Following the formation of NADH at 340 nm allowed the progress of the dehydrogenase reaction to be monitored. The Lineweaver–Burk plot shown in Fig. 9, obtained in the absence of inhibitor, afforded K_M and k_{cat} values consistent with literature values of type II human IMP dehydrogenase.[57]

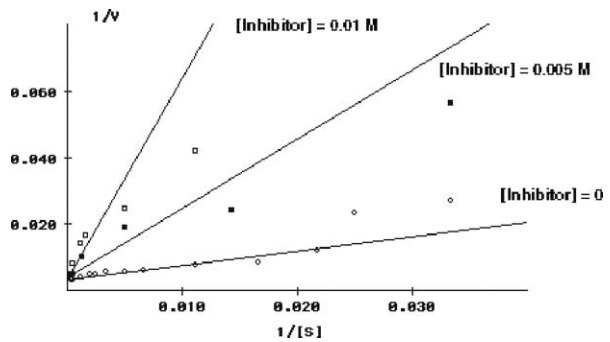

Fig. 9 Lineweaver–Burk plots for IMPDH-mediated oxidation of IMP (mM) in the presence of **2f**.

Also shown in Fig. 9 are Lineweaver–Burk plots obtained with type II IMP dehydrogenase in the presence of two concentrations of pyrrolobenzimidazole **2f**. These plots suggest that competitive inhibition of IMP dehydrogenase is occurring. However, these data are highly scattered perhaps due to irreversible inhibition (see reactions in Scheme 1). Recall that Lineweaver–Burk analysis assumes reversible inhibition. The Lineweaver–Burk K_i value is ~2 μM, which is the apparent dissociation of **2f** from the IMP dehydrogenase active site.

The conclusion of the IMPDH assays is that **2f** can interact with the IMPDH active site. Modelling studies suggest the **2a**,**e** could be accommodated by the IMPDH active site as well. Since inhibition is downstream to cellular uptake, a correlation with the IMPDH molecular target is not observed. Interactions of **LL-1** with the IMPDH active site cannot occur due to its larger size. However, enzymatic removal of a phenylalanine to afford **2f** will lead to IMPDH inhibition. Our next generation of analogues will possess a substituted phenylalanine and a terminal L-phenylalanine to facilitate uptake as well as enzymatic removal.

Conclusions

We report the successful design of a melanoma-specific cytotoxic agent **LL-1**. All four possible stereoisomers of **1** were prepared and screened; only the natural L, L-diphenylalanine stereoisomer showed melanoma specificity. Unfortunately, **LL-1** is highly toxic *in vivo* with mice deaths even at 1 mg kg^{-1} doses. The toxicity problem was solved by utilising the unnatural D-phenylalanine in the terminal position (**LD-1**). However, the melanoma specificity was lost, apparently because of the terminal D-phenylalanine. We postulate that the L-phenylalanines are removed enzymatically to afford a toxic PBI. The unnatural D-phenylalanine of **LD-1** prevents phenylalanine removal resulting in a maximum tolerated dose over 6 mg kg^{-1}.

The next step was to investigate substituted L-phenylalanines as alternatives to L-phenylalanine. The goal was to determine the L-phenylalanine substituent type that would optimise melanoma specificity and cytotoxicity. Matrix COMPARE and QSAR analyses revealed that the *para*-methoxy and the *para*-fluoro substituents (**2a** and **2b** respectively) resemble natural L-phenylalanine and possess enhanced potency against the melanoma cell lines. Currently we are evaluating second-generation substituted diphenylalanine PBI analogues *in vivo*.

COMPARE analysis of the unsubstituted phenylalanine analogues **2f** and **LL-1** revealed correlations with the respective molecular targets ABC-B5, a gene for a membrane transport protein, and ECM1, a gene for the Extracellular Matrix Protein 1. Correlations with these molecular targets are lost upon a change to the D-stereochemistry or the addition of a phenylalanine substituent.

The role of DT-diaphorase and IMP dehydrogenase were not obvious from these COMPARE analyses. Circumstantial evidence of the role of these molecular targets include the inhibition IMP dehydrogenase by **2f** reported herein and the well known reduction of simple PBIs by DT-diaphorase.[19,58] The involvement of either molecular target will require a monophenylalanine analogue (**2**) rather than the more sizable diphenylalanine analogue (**1**).

Therefore, another second-generation PBI analogue will possess a substituted phenylalanine and a terminal L-phenylalanine. We anticipate that the terminal phenylalanine will confer melanoma specificity and that its enzymatic removal will permit interaction with DT-diaphorase and IMP dehydrogenase.

Experimental

General

All analytically pure compounds were dried under high vacuum in a drying pistol over refluxing methanol. High resolution mass spectra and MALDI were run at Arizona State University. Melting points and decomposition points were determined with a Mel-Temp apparatus. All TLCs were performed on silica gel plates using a variety of solvent systems and a fluorescent indicator for visualization. IR spectra were taken as KBr pellets and only the strongest absorbances were reported. ^{1}H NMR spectra were obtained with a 300 or 500 MHz spectrometer. All chemical shifts are reported relative to TMS.

Synthesis

(3*S*)-6-Aziridinyl-2,3-dihydro-7-methyl-1*H*-3-(*N*-L-phenylalanyl-D-phenylalanylamino)-pyrrolo[1,2-*a*]benzimidazole-5,8-dione (LD-1). Yield: 17 mg (5.13%); mp: 132–135 °C (dec); TLC: [9 : 1 dichloromethane–methanol] R_f 0.26; ^{1}H NMR ($CDCl_3$) δ 7.92 (2H, br, amide NH), 7.30–7.0 (10H, 2 m, aromatic protons), 5.0 (1H, m, 3-methine proton), 4.65 (1H, br s, phenylalanine methine proton), 4.28 (1H, m, 1-methylene proton), 4.09 (1H, m, 1-methylene proton), 3.62 (1H, br s, phenylalanine methine proton), 2.91–3.18 (4H, m, phenylalanine methylene protons), 3.09 (1H, m, C(2) methylene proton), 2.61 (1H, m, C(2) methylene proton), 2.28 (4H, s, aziridine protons), 1.98 (3H, s, methyl protons); IR (thin film) 3357, 2929, 1623, 1462, 1404, 1381, 1234, 1125, 1082 cm^{-1}; MALDI: calculated for $C_{31}H_{32}N_6O_4 + H^+$ $(M + H)^+$ 553.256, found 553.251.

(3*S*)-6-Aziridinyl-2,3-dihydro-7-methyl-1*H*-3-(*N*-D-phenylalanyl-L-phenylalanylamino)-pyrrolo[1,2-*a*]benzimidazole-5,8-dione (DL-1). Yield: 16 mg (4.82%); mp: 110–112 °C (dec); TLC: [9 : 1 dichloromethane–methanol] R_f 0.51; ^{1}H NMR ($CDCl_3$) δ 8.2 (2H, br s, amide NH), 7.11–7.21 (10H, m, aromatic protons), 5.2 (1H, m, 3-methine proton), δ 4.83 (1H, br d, phenylalanine methine proton), 4.53 (1H, m, 1-methylene proton), 4.25 (1H, m, 1-methylene proton), 4.02 (1H, br s, phenylalanine methine proton), 2.82–3.16 (4H, m, phenylalanine methylene protons), 2.58 (1H, m, 2-methylene proton), 2.42 (1H, m, 2-methylene proton), 2.26 (4H, s, aziridine protons), 1.99 (3H, s, methyl protons); IR (thin film) 3260, 2931, 1644, 1518,1250 cm^{-1}; MALDI: calculated for $C_{31}H_{32}N_6O_4 + H^+$ $(M + H)^+$ 553.256, found 553.251.

(3*S*)-6-Aziridinyl-2,3-dihydro-7-methyl-1*H*-3-(*N*-D-phenylalanyl-D-phenylalanylamino)-pyrrolo[1,2-*a*]benzimidazole-5,8-dione (DD-1). Yield 15 mg (4.52%); mp: 148–150 °C (dec); TLC: [9 : 1 dichloromethane–methanol] R_f 0.40; ^{1}H NMR ($CDCl_3$): δ 8.64 (1H, d, J = 6.5 Hz, amide NH), 7.97 (1H, d, J = 6.5 Hz, amide NH), 7.14–7.32 (10H, m, aromatic protons), 4.87 (1H, q, J = 7.5 Hz, 3-methine proton), 4.11 (1H, m, 1-methylene proton), 3.97 (1H, m, 1-methylene proton), 3.69 (1H, doublet of doublets, J = 3 Hz, J = 6 Hz, phenylalanine methine proton), 3.03–3.14 (4H, m, phenylalanine methylene protons), 2.89 (1H, m, 2-methylene proton), 2.40 (1H, doublet of doublets, J = 11 Hz, J = 12.5 Hz, phenylalanine methine proton), 2.33 (2H, d, J = 6.5 Hz, aziridine protons), 2.30 (2H, d, J = 6 Hz, aziridine protons), 2.16 (1H, m, 2-methylene protons), 1.93 (3H, s, methyl protons); IR: (thin film) 3302, 2923, 1659, 1519, 1230 cm^{-1}; MALDI: calculated for $C_{31}H_{32}N_6O_4 + H^+$ $(M + H)^+$ 553.256, found 553.258.

General synthesis of intermediate 6

A solution of 1 mmol of *t*-Boc protected L-substituted-phenylalanine **5** in 15 mL of dry DCM was cooled to 0 °C. To this solution, 1.1 mL (1.1 mmol) of a 1 M solution of 1,3-dicyclohexylcarbodiimide (DCC) was added. The resulting mixture was stirred at 0 °C until the solution became cloudy. To this mixture was added 290 mg (0.93 mmol) of **4** and the mixture was removed from the ice bath and allowed to warm to room temperature and stirred for 2 h. The mixture was filtered, and the filtrate's purity was tested *via* TLC (9 : 1 dichloromethane–methanol). The dichloromethane was removed under reduced pressure to yield a white residue. The white residue contained a mixture of **6** and dicyclohexylurea side product. The dicyclohexylurea impurity was readily removed upon conversion to **7** in the next step. Recrystallisation of **6** from dichloromethane–hexane afforded pure material suitable for characterisation.

(3*S*)-6-Bromo-2,3-dihydro-7-methyl-5-nitro-3-[Boc-L-4-methoxyphenylalanyl]-1*H*-pyrrolo[1,2-*a*]benzimidazole (6a). 409 mg (75% yield); mp: 150–153 °C; TLC: [9 : 1 dichloromethane–methanol] R_f 0.60; ^{1}H NMR: (DMSO-d_6) 8.17 (1H, d, J ~ 8 Hz, urethane NH), 7.02 (2H, d, J = 8.5 Hz aromatic protons), ~7.0 (1H, s, 8-H), 6.87 (1H, d, J ~ 8 Hz, 9-amide proton), 6.8 (2H, d, J = 8.5 Hz aromatic protons & 1H, s, 8-H), 4.4 (1H, m, 3-methine proton), 3.9 & 4.2 (2H, 2 m, 1-methylene protons), 3.66 (3H, s, methoxy), 3.47 (1H, m, phenylalanine methine), 2.9 (1H, m, 2-methylene proton), 2.73 (1H, m, 2-methylene proton), 2.44 (3H, s, 6-Me), 2.5 & 2.9 (2H, 2 m, phenylalanine methylene protons), 1.28 (9H, s, *t*-Boc protons); IR (KBr pellet): 3332, 2932, 2855, 1676, 1631, 1537, 1447, 1368, 1307, 1225, 1165, 1052, 827 cm^{-1}; HRMS: Calculated 588.1458 for $C_{26}H_{31}{}^{79}BrN_5O_6$, found 588.1391, calculated 590.1437 for $C_{26}H_{31}{}^{81}BrN_5O_6$, found 590.1440.

(3*S*)-6-Bromo-2,3-dihydro-7-methyl-5-nitro-3-[Boc-L-4-fluorophenylalanyl]-1*H*-pyrrolo[1,2-*a*]benzimidazole (6b). 348 mg (65% yield); mp: 145–155 °C; TLC: [9 : 1 dichloromethane–methanol] R_f 0.60; ^{1}H NMR: (DMSO-d_6): 8.6 (1H, d, J ~ 8 Hz, amide NH), 7.8 (1H, s, 8-H), 6.9 (1H, d, J ~ 8 Hz, urethane NH), 7.0 & 7.38 (4H, 2d, J = 8.5 Hz aromatic protons), 5.3 (1H, m, 3-methine proton), 4.0 & 4.3 (2H, 2 m, 1-methylene protons), 3.95 (1H, m, phenylalanine methine proton), 2.7 & 3.0 (2H, 2 m, 2-methylene protons) 3.0 & 2.4 (2H, 2 m, phenylalanine methylene protons) 2.5 (3H, s, methyl), 1.28 (9H, s, *t*-Boc protons); IR: (KBr pellet) 3332, 2932, 2855, 1676, 1631, 1537, 1447, 1368, 1307, 1225, 1165, 1052, 827 cm^{-1}; HRMS Calculated 576.1258 for $C_{25}H_{28}{}^{79}BrFN_5O_5$, found 576.1266; Calculated 578.1237 for $C_{25}H_{28}{}^{81}BrFN_5O_5$, found 578.1289.

(3*S*)-6-Bromo-2,3-dihydro-7-methyl-5-nitro-3-[Boc-L-4-trifluoromethylphenylalanyl]-1*H*-pyrrolo[1,2-*a*]benzimidazole (6c). 431 mg (74% yield); mp: 185–195 °C TLC: [9 : 1 dichloromethane–methanol] R_f 0.60; ^{1}H NMR (DMSO) 8.7 (1H, d, J = 8 Hz, amide NH), 8.2 (1H, s, C8-H), 7.45 & 7.6 (4H, 2d, J = 8.5 Hz aromatic protons), 6.95 (1H, d, J = 8 Hz, urethane NH), 5.35 (1H, m, 3-methine proton), 4.0 (1H, m, phenylalanine methine proton), 4.0 & 4.3 (2H, 2 m, 1-methylene protons), 2.8–3.1 (2H, 2 m, 2-methylene protons) 2.4 & 2.95 (2H, 2 m, phenylalanine methylene protons), 2.5 (3H, s, methyl), 1.35 (9H, m, *t*-Boc protons); IR: (KBr pellet) 3420, 2933, 1676, 1527, 1367, 1327, 1166, 1124, 1067, 1020, 826; HRMS: Calculated 626.1226 for $C_{26}H_{28}{}^{79}BrF_3N_5O_5$, found 626.1260; Calculated 628.1206 for $C_{26}H_{28}{}^{81}BrF_3N_5O_5$, found 628.1200.

(3*S*)-6-Bromo-2,3-dihydro-7-methyl-5-nitro-3-[Boc-L-4-methylphenylalanyl]-1*H*-pyrrolo[1,2-*a*]benzimidazole (6d). 329 mg (62% yield); mp: 148–155 °C: TLC [9 : 1 dichloromethane–methanol] R_f 0.62; ^{1}H NMR (DMSO-d_6): 8.6 (1H, d, J = 8 Hz, amide NH), 7.8 (1H, s, C8-H), 7.05 & 7.18 (4H, 2d, J = 8.5 Hz aromatic protons), 6.8 (1H, d, J = 8 Hz, urethane NH), 5.3 (1H, m, 3-methine proton), 4.1 (1H, m, phenylalanine methine proton), 4.1 & 4.3 (2H, 2 m, 1-methylene protons), 2.95–2.75 (2H, 2 m, 2-methylene protons), 2.95 & 2.4 (2H, 2 m, phenylalanine methylene protons), 2.5 (3H, s,

methyl), 2.2 (3H, s, phenylalanine methyl), 1.28 (9H, m, *t*-Boc protons); IR: (KBr pellet) 3329, 2929, 2853, 1681, 1628, 1538, 1445, 1369, 1304, 1246, 1166, 1051, 877 cm^{-1}; HRMS: Calculated 572.1508 for $C_{26}H_{31}{}^{79}BrN_5O_5$, found 572.1535, calculated 574.1488 for $C_{26}H_{31}{}^{81}BrN_5O_5$, found 574.1489.

(3*S*)-6-Bromo-2,3-dihydro-7-methyl-5-nitro-3-[Boc-L-3-fluorophenylalanyl]-1*H*-pyrrolo[1,2-*a*]benzimidazole (6e). 387 mg (72% yield); mp: 183–190 °C; TLC: [9 : 1 dichloromethane–methanol] R_f 0.60; ^{1}H NMR (DMSO-d_6) 8.7 (1H, d, J ~ 8 Hz, amide NH), 8.2 (1H, s, 8-H), 7.8 (1H, d, J ~ 1 Hz, aromatic CH *ortho* to F), 7.1 & 7.3 (3H, 2 m, aromatic protons), 6.95 (1H, d, J ~ 8 Hz, urethane NH), 5.4 (1H, m, 3-methine proton), 4.1 (1H, m, phenylalanine methine proton), 4.0 & 4.3 (2H, 2 m, 1-methylene protons), 3.0 & 2.4 (2H, 2 m, phenylalanine methylene protons), 3.0 & 2.75 (2H, 2 m, 2-methylene protons), 2.51 (3H, m, methyl protons), 1.35 (9H, m, *t*-Boc protons); IR: (KBr pellet) 3330, 2932, 1676, 1629, 1527, 1450, 1367, 1250, 1166, 783 cm^{-1}; HRMS: Calculated 576.1258 for $C_{25}H_{28}BrFN_5O_5$, found 576.1237.

General synthesis of intermediate 7

To a degassed solution of 387 mg (0.67 mmol) of **6** in 50 mL of methanol was added 70 mg of 5% activated Pd/C. The resulting mixture was hydrogenated at 50 psi for 6 h. The catalyst was filtered off through Celite, and the methanol was removed from the filtrate under reduced pressure. A solution consisting of 80 mL of double distilled H_2O containing 1.2 g of potassium phosphate monobasic was added to the residue of the filtrate. To this solution was added 1 g of freshly prepared Fremy's salt, and the reaction stirred at room temperature for 1 h. The completed reaction was extracted with ethyl acetate until the organic extracts were colorless. The ethyl acetate was removed under reduced pressure to yield a brown residue of **7** along with trace deblocked (*t*-Boc) side product. This residue was dissolved in a minimum amount of chloroform and purified *via* silica gel chromatography employing ethyl acetate as the eluant. The yellow product was recrystallised from chloroform–hexane to afford analytically pure **7** as a yellow solid.

(3*S*)-2,3-Dihydro-7-methyl-3-[Boc-L-4-methoxyphenylalanyl]-1*H*-pyrrolo[1,2-*a*]benzimidazole-5,8-dione (7a). 45 mg (13% yield); mp: 118–123 °C; TLC: [9 : 1 dichloromethane–methanol] R_f 0.58; ^{1}H NMR (DMSO-d_6) 8.6 (1H, d, J = 8 Hz, amide NH), 7.18 & 6.8 (4H, 2d, J = 8.5 Hz aromatic protons), 6.8 (1H, d, J = 8 Hz, urethane NH), 6.6 (1H, s, 6-proton), 5.2 (1H, m, 3-methine proton), 4.05 (1H, m, phenylalanine methine proton), 4.3 & 4.1 (2H, 2 m, 1-methylene protons), 3.7 (3H, s, methoxy protons), 2.95 & 2.75 (2H, m & t respectively, J = 8 Hz, phenylalanine methylene protons), 2.9 & 2.3 (2H, 2 m, 2-methylene protons), 2.0 (3H, s, methyl protons), 1.30 (9H, m, *t*-Boc protons); IR, (KBr pellet) 3337, 2933, 2857, 1704, 1662, 1514, 1450, 1369, 1249, 1172, 1039, 827 cm^{-1}; HRMS Calculated: 495.2244 for $C_{25}H_{31}N_4O_6$, found 495.2234.

(3*S*)-2,3-Dihydro-7-methyl-3-[Boc-L-4-fluorophenylalanyl]-1*H*-pyrrolo[1,2-*a*]benzimidazole-5,8-dione (7b). 66 mg (23% yield); mp: 142–149 °C; TLC [9 : 1 dichloromethane–methanol] R_f 0.60; ^{1}H NMR (DMSO-d_6) 8.6 (1H, d, J = 8 Hz, amide NH), 7.25 & 7.05 (4H, 2 m, aromatic protons), 6.9 (1H, d, J = 8 Hz, urethane NH), 6.5 (1H, s, 6-proton), 5.2 (1H, m, 3-methine proton), 4.05 (1H, m, phenylalanine methine proton), 4.1 & 4.3 (2H, 2 m, 1-methylene protons), 2.95 & 2.7 (2H, 2 m, phenylalanine methylene protons), 2.9 & 2.4 (2H, 2 m, 2-methylene protons), 2.0 (3H, s, methyl protons), 1.35 (9H, m, *t*-Boc protons); IR (KBr pellet) 3425, 2930, 1665, 1512, 1369, 1160 cm^{-1}; HRMS Calculated: 483.2044 for $C_{25}H_{28}FN_4O_5$, found 483.2031.

(3*S*)-2,3-Dihydro-7-methyl-3-[Boc-L-4-trifluoromethylphenylalanyl]-1*H*-pyrrolo[1,2-*a*]benzimidazole-5,8-dione (7c). 50 mg (14% yield); mp 144–155 °C; TLC: [9 : 1 dichloromethane–methanol] R_f 0.55; ^{1}H NMR (DMSO-d_6): 8.6 (1H, d, J = 8 Hz, amide NH), 7.6 & 7.4 (4H, 2d, J = 8 Hz, aromatic protons), 7 (1H, d, J = 8 Hz, urethane NH), 6.55 (1H, s, 6-H), 5.2 (1H, m, 3-methine proton), 4.05 (1H, m, phenylalanine methine proton), 4.3 & 4.1 (2H, 2 m, 1-methylene protons), 3.05 & 2.8 (2H, 2 m, phenylalanine methylene protons), 3.0 & 2.35 (2H, 2 m, 2-methylene protons), 2.0 (3H, s, methyl protons), 1.35 (9H, m, *t*-Boc protons); IR (KBr pellet): 3426, 2931, 1658, 1525, 1327, 1248, 1164, 1124 cm^{-1}; HRMS Calculated: 533.2012 for $C_{26}H_{28}F_3N_4O_5$, found 533.2061.

(3*S*)-2,3-Dihydro-7-methyl-3-[Boc-L-4-methylphenylalanyl]-1*H*-pyrrolo[1,2-*a*]benzimidazole-5,8-dione (7d). 29 mg (9% yield); mp: 164–172 °C; TLC: [9 : 1 dichloromethane–methanol] R_f 0.62; ^{1}H NMR (DMSO-d_6): 8.6 (1H, d, J = 8 Hz, amide proton), 7.15 & 7.05 (4H, 2d, J = 8 Hz, aromatic protons), 6.8 (1H, d, J = 8 Hz, urethane NH), 6.57 (1H, s, 6-H), 5.2 (1H, m, 3-methine proton), 4.3 & 4.1 (2H, 2 m, 1-methylene protons), 4.1 (1H, m, phenylalanine methine proton), 2.95 & 2.75 (2H, 2 m, phenylalanine methylene protons), 2.95 & 2.30 (2H, 2 m, 2-methylene protons), 2.2 & 2.0 (6H, 2 s, methyl protons), 1.35 (9H, m, *t*-Boc protons); IR (KBr pellet) 3403, 2928, 1677, 1523, 1384, 1161 cm^{-1}; HRMS Calculated: 479.2294 for $C_{26}H_{31}N_4O_5$, found 479.2295.

(3*S*)-2,3-Dihydro-7-methyl-3-[Boc-L-3-fluorophenylalanyl]-1*H*-pyrrolo[1,2-*a*]benzimidazole-5,8-dione (7e). 71 mg (22% yield); mp: 143–152 °C; TLC [9 : 1 dichloromethane–methanol]: R_f 0.58; ^{1}H NMR (DMSO-d_6): 8.6 (1H, d, J = 8 Hz, amide proton), 7.25 & 7.05 (4H, 2 m, aromatic protons), 6.95 (1H, d, J = 8 Hz, urethane NH), 6.57 (1H, s, 6-H), 5.2 (1H, m, 3-methine proton), 4.05 (1H, m, phenylalanine methine proton), 4.3 & 4.1 (2H, 2 m, 1-methylene protons), 2.95 & 2.75 (2H, 2 m, phenylalanine methylene protons), 2.9 & 2.30 (2H, 2 m, 2-methylene protons), 2.0 (3H, s, 7 methyl protons), 1.35 (9H, m, *t*-Boc protons); IR (KBr pellet): 3331, 2931, 2854, 1663, 1528, 1520, 1368, 1249, 1160 cm^{-1}; HRMS Calculated: 483.2044 for $C_{25}H_{28}FN_4O_5$, found 483.2048.

General synthesis of 2 from intermediate 7

This transformation was carried out in two steps: removal of the *t*-Boc protecting group with trifluoroacetic acid (TFA) followed by aziridination. A solution of 0.1 mmol of **7** in 10 mL and TFA (0.25 mL) was stirred at room temperature. The reaction was monitored by TLC (9 : 1 dichloromethane–methanol). Upon completion, the reaction solvent was removed under reduced pressure. The residue was dissolved in 15 mL of anhydrous methanol and cooled to 0 °C. To this mixture was added 0.4 mL of aziridine and stirring continued at 0 °C for 30 min. The reaction mixture was then allowed to warm to room temperature and stirred for 3 h. The solvent was removed under reduced pressure and

the residue was dissolved in a minimum amount of chloroform which was spotted onto a preparatory TLC plate employing 9 : 1 dichloromethane and methanol. The bright red band was scraped off the plate and extracted with ethyl acetate. The ethyl acetate was removed under reduced pressure, and **2** was recrystallized from chloroform–hexane. The yield of purified product ranged from 2 to 7%.

(3*S*)-6-Aziridinyl-2,3-dihydro-7-methyl-3-(L-*p*-methoxyphenyl-alanylamino)-1*H*-pyrrolo[1,2-*a*]benzimidazole-5,8-dione (2a). Yield: 15 mg (4.59%); mp 145–146 °C (dec); TLC [dichloromethane–methanol (90 : 10)]: R_f 0.39; ^{1}H NMR ($CDCl_3$) δ 8.29 (1H, br s, amide NH), 7.11 (2H, d, J = 8.5 Hz aromatic protons), 6.82 (2H, d, J = 8.5 Hz aromatic proton), 5.21 (1H, m, 3-methine proton), 4.34 (1H, m, 1-methylene proton), 4.12 (1H, m, 1-methylene proton), 3.77 (3H, s, methoxy protons), 3.68 (1H, br s, phenylalanine methine proton), 3.12 (2H, dd, J = 10.5 Hz, J = 3.5 Hz, phenylalanine methylene proton), 2.74 (1H, m, 2-methylene proton), 2.51 (1H, m, 2-methylene proton), 2.33 (4H, s, aziridine), 2.02 (3H, s, methyl protons); IR (thin film) 3311, 2924, 2854, 1672, 1581, 1512, 1461, 1378, 1302, 1247, 1179, 1139, 1033, 812 cm^{-1}; MALDI: calculated for $C_{23}H_{25}N_5O_4$ + H^+ $(M + H)^+$ 436.198, found 436.195; calculated for $C_{23}H_{25}N_5O_4$ + Na^+ $(M + Na)^+$ 458.180, found 458.173.

(3*S*)-6-Aziridinyl-2,3-dihydro-7-methyl-3-(L-*p*-fluorophenyl-alanylamino)-1*H*-pyrrolo[1,2-*a*]benzimidazole-5,8-dione (2b). Yield: 21 mg (6.62%); mp: 275–276 °C (dec); TLC: [9 : 1 dichloromethane–methanol] R_f 0.33; ^{1}H NMR ($CDCl_3$): δ 8.16 (1H, br s, amide NH), 7.06 (2H, dd, J = 7.8 Hz, J = 5.4 Hz aromatic protons), 6.88 (2H, dd, J = 8.7 Hz, J = 8.1 Hz aromatic protons), 5.11 (1H, m, 3-methine proton), 4.23 (1H, m, 1-methylene proton), 4.05 (1H, m, 1-methylene proton), 3.59 (1H, dd, J = 5.40 Hz, J = 5.10 Hz, phenylalanine methine proton), 3.05 (2H, m, phenylalanine methylene proton), 2.71 (1H, m, 2-methylene proton), 2.40 (1H, m, 2-methylene proton), 2.24 (4H, s, aziridine), 1.93 (3H, s, methyl protons); IR (thin film): 3328, 2924, 2854, 1675, 1639, 1577, 1511, 1378, 1339, 1313, 1221, 1139, 1099 cm^{-1}; MALDI: calculated for $C_{22}H_{22}N_5O_3F$ + H^+ $(M + H)^+$ 424.178, found 424.181; calculated for $C_{22}H_{22}N_5O_3F$ + Na^+ $(M + Na)^+$ 446.161, found 446.161.

(3*S*)-6-Aziridinyl-2,3-dihydro-7-methyl-3-(L-*p*-trifluoromethyl-phenylalanylamino)-1*H*-pyrrolo[1,2-*a*]benzimidazole-5,8-dione (2c). Yield: 8 mg (2.25%); mp: 182–184 °C (dec); TLC [9 : 1 dichloromethane–methanol]: R_f 0.28; ^{1}H NMR ($CDCl_3$): δ 8.45 (1H, br s, amide NH), 7.55 (2H, d, J = 6.5 Hz aromatic protons), 7.36 (2H, d, J = 7.5 Hz aromatic protons), 5.20 (1H, br s, 3-methine proton), 4.34 (1H, m, 1-methylene proton), 4.12 (1H, m, 1-methylene proton), 3.84 (1H, br s, *p*-trifluoromethyl phenylalanine methine proton), 3.28 (1H, d, J = 12.5 Hz, trifluoromethyl phenylalanine methylene proton), 3.09 (1H, d, J = 7.5 Hz, trifluoromethyl phenylalanine methylene proton), 2.93 (1H, m, 2-methylene proton), 2.52 (1H, m, 2-methylene proton), 2.34 (4H, s, aziridine), 2.02 (3H, s, methyl protons); IR (thin film): 3325, 2922, 2853, 1724, 1553, 1500, 1461, 1374, 1319, 1191, 1038 cm^{-1}; MALDI: calculated for $C_{23}H_{22}N_5O_3F_3$ + H^+ $(M + H)^+$ 474.175, found 474.170; calculated for $C_{23}H_{22}N_5O_3F_3$ + Na^+ $(M + Na)^+$ 496.156, found 496.151.

(3*S*)-6-Aziridinyl-2,3-dihydro-7-methyl-3-(L-4-methylphenyl-alanylamino)-1*H*-pyrrolo[1,2-*a*]benzimidazole-5,8-dione (2d). Yield: 22 mg (7.00%); mp: 149–150 °C (dec); TLC [9 : 1 dichloromethane–methanol]: R_f 0.48; ^{1}H NMR ($CDCl_3$) δ 8.24 (1H, br s, amide NH), 6.99 (4H, m, aromatic protons), 5.12 (1H, q, J = 7.20 Hz, 3-methine proton), 4.20–4.31 (1H, m, 1-methylene proton), 3.99–4.08 (1H, m, 1-methylene proton), 3.60–3.70 (1H, dd, J = 3.9 Hz, J = 3.6 Hz, phenylalanine methine proton), 3.05–3.12 (1H, dd, J = 3.9 Hz, J = 3.6 Hz, phenylalanine methylene proton), 2.973–3.03 (1H, dd, J = 4.80 Hz, J = 3.3 Hz, phenylalanine methylene proton), 2.62–2.70 (1H, m, 2-methylene proton), 2.4–2.5 (1H, m, 2-proton), 2.24 (4H, s, aziridine), 2.20 (3H, s, methyl protons), 1.94 (3H, s, methyl protons). IR (thin film) 3324, 2924, 1675, 1583, 1518, 1486, 1379, 1313, 1250, 1140, 1098, 1032, 991, 783 cm^{-1}; MALDI: calculated for $C_{23}H_{25}N_5O_3$ + H^+ $(M + H)^+$ 420.203, found 420.208; calculated for $C_{23}H_{25}N_5O_3$ + Na^+ $(M + Na)^+$ 442.186, found 442.186.

(3*S*)-6-Aziridinyl-2,3-dihydro-7-methyl-3-(L-*m*-fluorophenyl-alanylamino)-1*H*-pyrrolo[1,2-*a*]benzimidazole-5,8-dione (2e). Yield: 23 mg (7.24%); mp: 294–295 °C (dec); TLC [9 : 1 dichloromethane–methanol]: R_f 0.35; ^{1}H NMR ($CDCl_3$): δ 8.36 (1H, br s, amide NH), 7.17 (1H, d, J = 7.50 Hz, aromatic protons), 6.93 (1H, d, J = 7.50 Hz, aromatic proton), 6.82–6.88 (2H, m, J = 9.3 Hz, J = 8.7 Hz aromatic protons), 5.14 (1H, br s, 3-methine proton), 4.23–4.32 (1H, m, 1-methylene proton), 4.00–4.10 (1H, m, 1-methylene proton), 3.71 (1H, s, phenylalanine methine proton), 3.01–3.17 (2H, m, phenylalanine methylene proton), 2.81 (1H, m, 2-methylene proton), 2.47 (1H, m, 2-methylene proton), 2.28 (4H, s, aziridine), 1.95 (3H, s, methyl protons); IR (thin film) 3329, 2926, 1675, 1639, 1582, 1518, 1378, 1312, 1250, 1139, 1072, 1032 cm^{-1}; MALDI: calculated for $C_{22}H_{22}N_5O_3F$ + H^+ $(M + H)^+$ 424.178, found 424.180; calculated for $C_{22}H_{22}N_5O_3F$ + Na^+ $(M + Na)^+$ 446.161, found 446.163.

In vivo studies

Either male or female SCID mice were implanted with the xenograft tumour model for human lung (NCI-H460). Compound **LL-1** was administrated intraperitoneally at doses of 1, 3, and 5 mg kg^{-1} at 4 day intervals for a total of 6 doses. Each mL of the solvent for **LL-1** consisted of 2 mg citric acid, 30 mg benzyl alcohol, 80 mg polyoxyethylene sorbitan monooleate (tween 80), 650 mg polyethylene glycol 300 and 30.5% ethanol (w/w). The tumour size, body weight and signs of overt animal toxicity after **LL-1** injection were monitored for 25 days.

Acute toxicity assays

A concentration of **LD-1** was prepared, consistent with administration of 400 mg kg^{-1} intraperitoneally, in a volume of 1 mL. Treat each SCID mouse with a single dose of 400, 200, and 100 mg kg^{-1} (1 mL, 0.5 mL, and 0.25 mL/mouse). The body weight and strain of mouse used should be consistent with that to be used in the subsequent antitumor evaluation protocols. Hold the animals for a period of 14 days observing for morbidity (body weight loss) and mortality. If the mice do not survive for 14 days, administer a 50% lower dose to a single mouse and continue this process (50 mg kg^{-1}, 25 mg kg^{-1}, 12.5 mg kg^{-1}, *etc.*) until a tolerated dosage

is determined. Use the maximum tolerated dosage as the basis for selecting doses for antitumor drug evaluations.

Hollow fibre assays[48,49]

Mice are treated with either a high or a low dose using a QD × 4 schedule (four daily treatments) administered intraperitoneally. Altogether, twelve cell lines are studied resulting in 48 possible test combinations (12 cell lines × 2 sites × 2 doses). A score of two is given to each test in which there is a % T/C of 50 or less (tumor mass 50% or less than the control). Thus the highest possible score is a 96, but the typical score is only 5 and the highest score achieved so is a 64. The score is broken down into a intraperitoneal (IP) and a subcutaneous (SC) score. A good SC score (≥ 8) indicates that the drug is able to get to the tumour site (subcutaneous) from a distant site (intraperitoneal) of injection.

QSAR calculations

Multivarible regression analysis was carried out using GraphPad InStat. Substituent constants were obtained from Hansch and Leo.[53]

IMP dehydrogenase inhibition assays

These assays were carried out as previously described by this laboratory.[59] The IMP dehydrogenase activity was measured at 340 nm in 1.0 cm path length cuvette maintained at 30 °C in a CARY-14 UV/VIS spectrophotometer. The final assay volume was set to 1.0 mL and contained 100 mM Tris-HCl (pH 8.0), 100 mM KCl, 5 mM mercaptoethanol, 3 mM EDTA, 100 µL type II IMP dehydrogenase, 1 mM DTT, 0.40 mM IMP, and 0.30 mM NAD^+. The solution mixture, including everything except the enzyme, was placed in the spectrophotometer and was allowed to temperature equilibrate for 5 min. The dehydrogenase reaction was initiated upon addition of type II IMP dehydrogenase and formation of NADH was monitored for 30 min. Next, to determine the K_m value concentration of IMP was varied from 0.25 mM to 25 mM and corresponding rates in terms of optical density were obtained. To determine activity of type II IMP dehydrogenase in the presence of potential inhibitors, the experiment was repeated in the presence of 0.01 and 0.005 mM **2f**.

Acknowledgements

We wish to thank the Arizona Biomedical Research Commission for their generous support.

References

1 D. T. Ross, U. Scherf, M. B. Eisen, C. M. Perou, C. Rees, P. Spellman, V. Iyer, S. S. Jeffrey, M. Van De Rijn, M. Waltham, A. Pergamenschikov, J. C. E. Lee, D. Lashkari, D. Shalon, T. G. Myers, J. N. Weinstein, D. Botstein and P. O. Brown, *Nat. Genet.*, 2000, **24**, 227.
2 P. L. Gutierrez, *Free Radical Biol. Med.*, 2000, **29**, 263.
3 A. M. Rauth, Z. Goldberg and V. Misra, *Oncol. Res.*, 1997, **9**, 339.
4 M. D. Garrett and P. Workman, *Eur. J. Cancer*, 1999, **35**, 2010.
5 I. J. Stratford and P. Workman, *Anti-Cancer Drug Des.*, 1998, **13**, 519.
6 P. Workman, *Oncol. Res.*, 1994, **6**, 461.
7 R. W. Franck and M. Tomasz, The Chemistry of Mitomycins, in *The Chemistry of Antitumor Agents*, ed. D. E. Wilman, Blackie & Sons, Ltd., Glasgow, Scotland, 1990, 379394.
8 D. Siegel, H. Beall, C. Senekowitsch, M. Kasai, H. Arai, N. W. Gibson and D. Ross, *Biochemistry*, 1992, **31**, 7879.
9 P. Schiltz and H. Kohn, *J. Am. Chem. Soc.*, 1993, **115**, 10510.
10 J. Cummings, *Drug Resist. Updates*, 2000, **3**, 143.
11 W. Ping, S. Yang, Z. Lixia, H. Hanping and Z. Xiang, *Curr. Med. Chem.*, 2005, **12**, 2893.
12 K. U. Schallreuter and J. M. Wood, *Biochem. Biophys. Res. Commun.*, 1999, **262**, 423.
13 I. Islam and E. B. Skibo, *J. Org. Chem.*, 1990, **55**, 3195.
14 E. B. Skibo and W. G. Schulz, *J. Med. Chem.*, 1993, **36**, 3050.
15 W. G. Schulz, E. Islam and E. B. Skibo, *J. Med. Chem.*, 1995, **38**, 109.
16 E. B. Skibo, *Curr. Med. Chem.*, 1996, **2**, 900.
17 E. B. Skibo, I. Islam, W. G. Schulz, R. Zhou, L. Bess and R. Boruah, *Synlett*, 1996, 297.
18 R. Zhou and E. B. Skibo, *J. Med. Chem.*, 1996, **39**, 4321.
19 E. S. Skibo, S. Gordon, L. Bess, R. Boruah and J. Heileman, *J. Med. Chem.*, 1997, **40**, 1327.
20 W. A. Craigo, B. W. LeSueur and E. B. Skibo, *J. Med. Chem.*, 1999, **42**, 3324.
21 X. Huang, A. Suleman and E. B. Skibo, *Bioorg. Chem.*, 2000, **28**, 324.
22 A. Ghodousi, X. Huang, Z. Cheng and E. B. Skibo, *J. Med. Chem.*, 2004, **47**, 90.
23 R. I. Christopherson, S. D. Lyons and P. K. Wilson, *Acc. Chem. Res.*, 2002, **35**, 961.
24 A. G. Zimmermann, J. J. Gu, J. Laliberte and B. S. Mitchell, Inosine-5′-monophosphate dehydrogenase: Regulation of expression and role in cellular proliferation and T lymphocyte activation, in *Progress in Nucleic Acid Research and Molecular Biology, Vol. 61*, ed. K. Moldave, Academic Press Inc., San Diego, 1998, 181209.
25 Y. Natsumeda and S. F. Carr, *Ann. N. Y. Acad. Sci.*, 1993, **696**, 88.
26 P. Franchetti, L. Cappellacci and M. Grifantini, *Farmaco*, 1996, **51**, 457.
27 K. W. Pankiewicz, *Expert Opin. Ther. Pat.*, 2001, **11**, 1161.
28 N. Minakawa and A. Matsuda, *Curr. Med. Chem.*, 1999, **6**, 615.
29 K. W. Pankiewicz, S. E. Patterson, P. L. Black, H. N. Jayaram, D. Risal, B. M. Goldstein, L. J. Stuyver and R. F. Schinazi, *Curr. Med. Chem.*, 2004, **11**, 887.
30 K. Gharehbaghi, W. Grunberger and H. N. Jayaram, *Curr. Med. Chem.*, 2002, **9**, 743.
31 J. Jain, S. J. Almquist, D. Shlyakhter and M. W. Harding, *J. Pharm. Sci.*, 2001, **90**, 625.
32 W. Markland, T. J. McQuaid, J. Jain and A. D. Kwong, *Antimicrob. Agents Chemother.*, 2000, **44**, 859.
33 M. D. Sintchak and E. Nimmesgern, *Immunopharmacology*, 2000, **47**, 163.
34 L. A. Sorbera, J. S. Silvestre, J. Castaner and L. Martin, *Drugs Future*, 2000, **25**, 809.
35 Y. Jin, H.-Y. Li, L.-P. Lin, J. Tan, J. Ding, X. Luo and Y.-Q. Long, *Bioorg. Med. Chem.*, 2005, **13**, 5613.
36 S. H. Watterson, T. G. M. Dhar, S. K. Ballentine, Z. Q. Shen, J. C. Barrish, D. Cheney, C. A. Fleener, K. A. Rouleau, R. Townsend, D. L. Hollenbaugh and E. J. Iwanowicz, *Bioorg. Med. Chem. Lett.*, 2003, **13**, 1273.
37 T. D. Colby, K. Vanderveen, M. D. Strickler, G. D. Markham and B. M. Goldstein, *Proc. Natl. Acad. Sci. U. S. A.*, 1999, **96**, 3531.
38 E. B. Skibo and R. B. Meyer, *J. Med. Chem.*, 1981, **24**, 1155.
39 T. D. Colby, K. Vanderveen, M. D. Strickler, G. D. Markham and B. M. Goldstein, *Proc. Natl. Acad. Sci. U. S. A.*, 1999, **96**, 3531.
40 D. K. Paull, R. H. Shoemaker, L. Hodes, A. Monks, D. A. Scudiero, L. Rubinstein, J. Plowman and M. R. Boyd, *J. Natl. Cancer Inst.*, 1989, **81**, 1088.
41 D. S. Swaffar, C. M. Ireland and L. R. Barrows, *Anti-Cancer Drugs*, 1994, **5**, 15.
42 E. B. Skibo and C. Xing, *Biochemistry*, 1998, **37**, 15199.
43 I. Islam, E. B. Skibo, R. T. Dorr and D. S. Alberts, *J. Med. Chem.*, 1991, **34**, 2954.
44 E. B. Skibo, I. Islam, M. J. Heileman and W. G. Schulz, *J. Med. Chem.*, 1994, **37**, 78.
45 M. R. Boyd, Status of the NCI Preclinical Antitumor Drug Discovery Screen, in *Principles and Practices of Oncology (PPO), 3 ed.*, ed. V. T. DeVita, S. Hellman and S. A. Rosenberg, J. B. Lippincott, Phildelphia, Pa., USA, 1989, Vol. 3, 112.
46 M. R. Boyd and K. D. Paull, *Drug Dev. Res.*, 1995, **34**, 91.
47 A. Monks, D. A. Scudiero, G. S. Johnson, K. D. Paull and E. A. Sausville, *Anti-Cancer Drug Des.*, 1997, **12**, 533.

48 M. G. Hollingshead, M. C. Alley, R. F. Camalier, B. J. Abbott, J. G. Mayo, L. Malspeis and M. R. Grever, *Life Sci.*, 1995, **57**, 131.
49 M. G. Hollingshead, J. Plowman, M. Alley, J. Mayo and E. Sausville, Relevance of Tumor Models in Anticancer Drug Development, in *Contrib. Oncol.*, Krager Verlag, Germany, 1999, 109120.
50 H. H. Sedlacek, J. Czech, R. Naik, G. Kaur, P. Worland, M. Losiewicz, B. Parker, B. Carlson, A. Smith, A. Senderowicz and E. Sausville, *Int. J. Oncol.*, 1996, **9**, 1143.
51 L. Hodes, K. Paull, A. Koutsoukos and L. Rubinstein, *J. Biopharm. Stat.*, 1992, **2**, 31.
52 C. Hansch, *Acc. Chem. Res.*, 2002, **2**, 232.
53 C. Hansch and A. Leo, '*Substituent Constants For Correlation Analysis in Chemistry and Biology*', Wiley-Interscience, 1979.
54 S. Heimerl, A. K. Bosserhoff, T. Langmann, J. Ecker and G. Schmitz, *Melanoma Res.*, 2007, **17**, 265.
55 N. Y. Frank, A. Margaryan, Y. Huang, T. Schatton, A. M. Waaga-Gasser, M. Gasser, M. H. Sayegh, W. Sadee and M. H. Frank, *Cancer Res.*, 2005, **65**, 4320.
56 L. Wang, J. Yu, J. Ni, X.-M. Xu, J. Wang, H. Ning, X.-F. Pei, J. Chen, S. Yang, C. B. Underhill, L. Liu, J. Liekens, J. Merregaert and L. Zhang, *Cancer Lett.*, 2003, **200**, 57.
57 J. E. McLean, N. Hamaguchi, P. Belenky, S. E. Mortimer, M. Stanton and L. Hedstrom, *Biochem. J.*, 2004, **379**, 243.
58 A. Suleman and E. B. Skibo, *J. Med. Chem.*, 2002, **45**, 1211.
59 M. E. Pugh and E. B. Skibo, *Comp. Biochem. Physiol.*, 1993, **105B**, 381.